

# A lightweight thermal heat switch for redundant cryocooling on satellites

M. Dietrich<sup>a,\*</sup>, A. Euler<sup>a</sup>, G. Thummes<sup>a,b</sup>

<sup>a</sup>*TransMIT-Centre of Adaptive Cryotechnology and Sensors, 35392 Giessen, Germany*

<sup>b</sup>*Institute of Applied Physics, University of Giessen, 35392 Giessen, Germany*

---

## Abstract

A previously designed cryogenic thermal heat switch for space applications has been optimized for low mass, high structural stability, and reliability. The heat switch makes use of the large linear thermal expansion coefficient (CTE) of the thermoplastic UHMW-PE for actuation. A structure model, which includes the temperature dependent properties of the actuator, is derived to be able to predict the contact pressure between the switch parts. This pressure was used in a thermal model in order to predict the switch performance under different heat loads and operating temperatures. The two models were used to optimize the mass and stability of the switch. Its reliability was proven by cyclic actuation of the switch and by shaker tests.

**Keywords:** Passive heat switch, Pulse tube cryocooler, CTE, Space cryogenics, Reliability, Redundancy

---

## 1. Introduction

Redundancy concepts are of vital importance for long term satellite missions [1]. If cryocoolers are involved, several methods are possible to achieve redundancy [2]. One method is to use two identical cryocoolers; one active and one in stand-by operation. In the simplest case, both cryocoolers are directly connected to the cooling load. However, this approach has the drawback that the active cryocooler has to carry the thermal load introduced by the stand-by cryocooler, which usually requires an increased power input to the active part or even a larger cooler model. An increased power input usually lowers the reliability of the system while a larger cryocooler model increases the total system mass. An alternative is to use thermal heat switches [3], which connect each cooler to a common heat load (e.g. an infrared detector). This method can reduce the thermal load of the stand-by cryocooler significantly.

The passively operated thermal heat switch was developed in a previous project where it was able to demonstrate that the design principle works [4]. The switch makes use of the very high coefficient of thermal expansion (CTE) of the thermoplastic Ultra-High Molecular Weight Polyethylene (UHMW-PE). The high CTE allows for a relative large gap width of 80  $\mu\text{m}$  in the open state, which facilitates the manufacturing and enhances the reliability. This first generation heat switch showed an on-state thermal conductance of 1000 mW/K at 100 K and an off-state thermal conductance of 3 mW/K between 80 and 260 K. However,

---

<sup>\*</sup>©2017. This manuscript version is made available under the CC-BY-NC-ND 4.0 license <http://creativecommons.org/licenses/by-nc-nd/4.0/>

<sup>\*</sup>Corresponding author at: TransMIT-Centre of Adaptive Cryotechnology and Sensors, Heinrich-Buff-Ring 16, 35392 Giessen, Germany. Tel.: +49 641 99 33462

Email address: [dietrich@transmit.de](mailto:dietrich@transmit.de) (M. Dietrich)

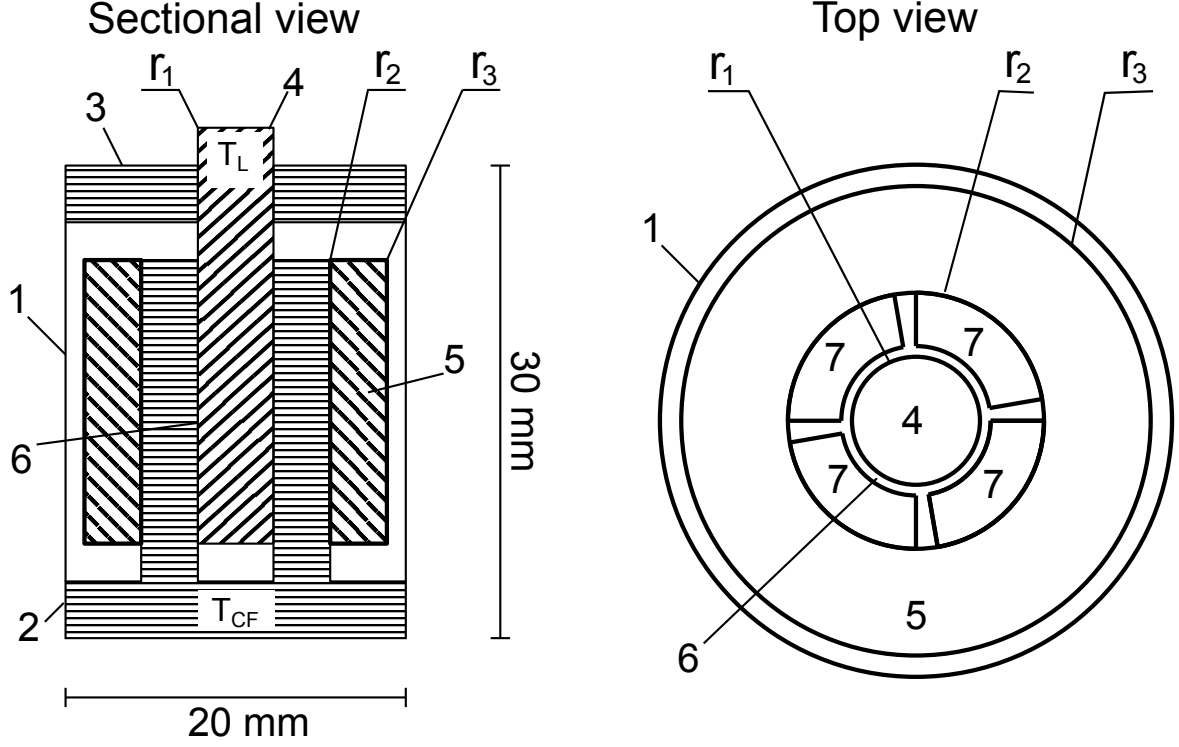


Figure 1: Schematic view of the heat switch (not to scale). 1: Connector (titanium alloy tube), 2: lower switch part with jaws (7) and cold flange ( $T_{CF}$ ) made of aluminium alloy, 3: shaft holder (epoxy or aluminium), 4: upper switch part with shaft and connection to load ( $T_L$ ) made of aluminum alloy, 5: actuator tube (UHMW-PE), 6: small gap.

with a mass of 250 g, the switch was still too heavy to be launched into space. Additionally, it underwent only limited reliability testing, especially of the poorly understood creep behavior of the actuator material. Lastly, the first generation heat switch performance was adversely impacted by shaker tests.

For further improvement of the switch, a structural and a thermal model were created with the aim to reduce the mass and to increase the stability simultaneously. A reduction in on-state conductance to about 500 mW/K at 100 K was tolerable for the intended cooling of infrared detectors.

## 2. Models and changes in switch design

The principle design of the heat switch, as shown in Fig. 1, is described in more detail in [4]. The thermal model is used to estimate the thermal conductance in the on- and off-state. In the off-state, the main heat flow path is along the mechanical connector (1) of the two switch parts (2, 4) shown on the left in Fig. 1. In the old design, this connector consisted of four thin-walled stainless-steel capillary tubes, which only provided a small structural support. These capillary tubes were replaced by a single thin-walled tube made of titanium alloy, which has a lower thermal conduction than the previous four stainless steel capillaries. To further reduce the thermal conductance in the off-state, the shaft holder material (3) was changed from copper to a low outgassing epoxy. Furthermore, the switch width was reduced in order to lower the total mass. As a consequence of this shrink, the gap width had to be reduced from 80  $\mu\text{m}$  to 70  $\mu\text{m}$ . By these

measures, the heat conductance in off-state was reduced from the early 2 mW/K (between 100 and 220 K) to 1.6 mW/K. However, the thermal model predicted a somewhat higher off-state conductance of 2.3 mW/K. This higher value is probably due to the thermal contact resistances between the various parts of the real switch, which were not included in the model.

To be able to calculate the thermal conductance in the on-state, the thermal model needs information about the pressure between the switch contact areas. A structural model was therefore developed, which includes the temperature dependent properties of the materials used, especially the coefficients of thermal expansion. With regard to the switch geometry, the contact pressure is then calculated using Hooke's law as

$$P(T) = \frac{E_{al}E_{pe}(r_2 - r_3)^2(\varepsilon_{al}(T) - \varepsilon_{pe}(T))}{(\nu_{al} - 1)(E_{al}\nu_{pe}(r_2^2 + r_3^2) - (E_{al} + E_{pe})(r_2 - r_3)^2)}, \quad (1)$$

where  $E$ ,  $\varepsilon$ , and  $\nu$  are the creep modulus, thermal expansion at temperature  $T$ , and Poisson's ratio, respectively. The radii  $r_2$  and  $r_3$  are indicated in Fig. 1 and denote the outer radius of the jaws and the actuator, respectively. The indices "al" and "pe" stand for the different switch materials aluminium and UHMW-PE, respectively. Due to the lack of available data, the CTE of the UHMW-PE actuator material was measured in advance, which revealed a contraction from 300 K to 100 K of 2.1% (Al 6061-T6: 0.38%). The calculated contact pressure at 100 K is a bit lower than in the first generation design (3.9 MPa vs. 4.2 MPa, primarily due to the reduction of the switch dimensions. The contact conductance  $h_c$  was first estimated from [5] and later measured using the real switch. The contact conductance  $h_c$  was calculated from the experimental results using a model derived from the Fourier-law:

$$\dot{Q} = \frac{\Delta T k_s h_c A}{(r_1/2 + (r_2 - r_1)/2)h_c + k_s}, \quad (2)$$

where  $\dot{Q}$  is the heat load,  $r_1$  and  $r_2$  are the radii as indicated in Fig. 1,  $A$  is the contact area between jaws and shaft,  $\Delta T = T_L - T_{CF}$  is the temperature difference between the connection to the load (4) and cold flange (2), and  $k_s$  is the mean thermal conductivity of aluminium of the jaws and shaft (2, 4).

Measurements of the contact conductance were performed using an in-house made coaxial pulse-tube cryocooler (model PT08) employing an SL-400 compressor from AIM GmbH, Heilbronn, Germany [6]. The experimental setup with the heat switch mounted in the cold flange of the PT08 is shown in Fig. 2.

The experimental data were then fitted using a power law from [5]:

$$h_c = 1.25 * k_s \left(\frac{m}{\sigma}\right) \left(\frac{P}{H}\right)^{0.95} \propto a * P^{0.95}. \quad (3)$$

The single fit parameter  $a$  includes the difficult to determine properties of the switch contact surface, namely the RMS surface roughness  $\sigma$ , the RMS slope of the asperities  $m$ , and the microhardness  $H$ , which are assumed to be constant in the relevant temperature range between 100 and 200 K. The temperature dependent contact pressure  $P$  was calculated from the structural model (see Eq. 1). Fig. 3 compares the thermal conductance from experimental data with the contact conductance calculated from Eq. 3. The fitted model shows a good agreement with the experimental data. However, the thermal contact conductance  $h_c$  is an order of magnitude lower than predicted by [5]. One reason is that the microhardness  $H$  increases with lower temperature leading to a smaller contact conductance (see Eq. 3 and [7]). Another reason is

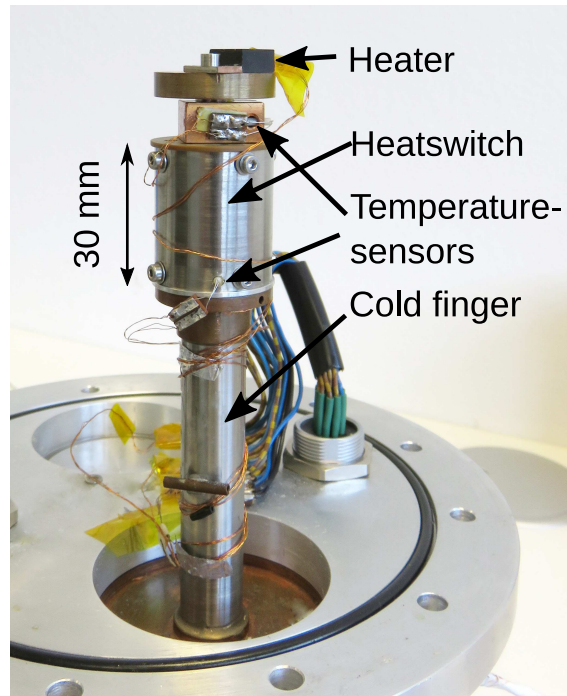


Figure 2: Photo of the experimental setup.

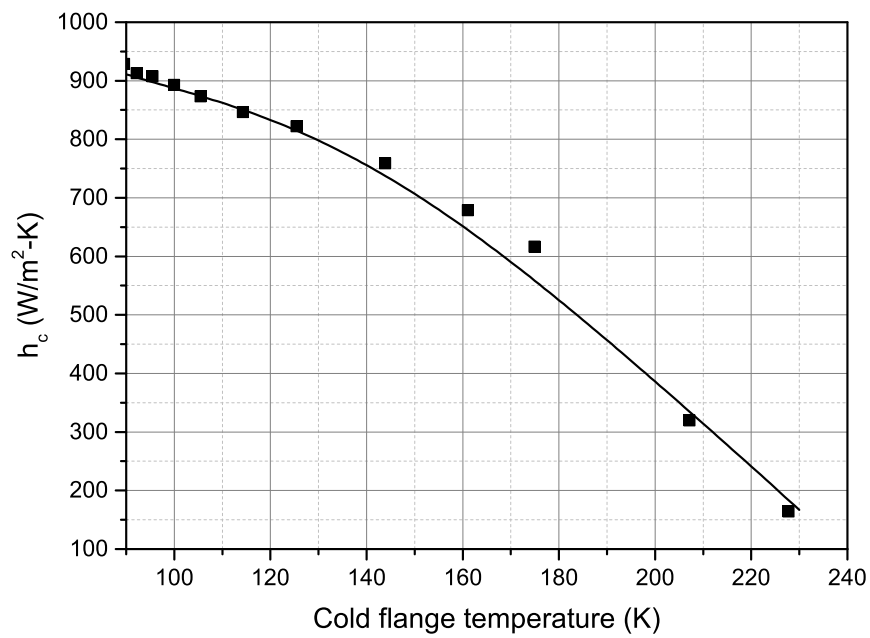


Figure 3: Measured (squares) and fitted contact conductance of the heat switch as function of the cold flange temperature.

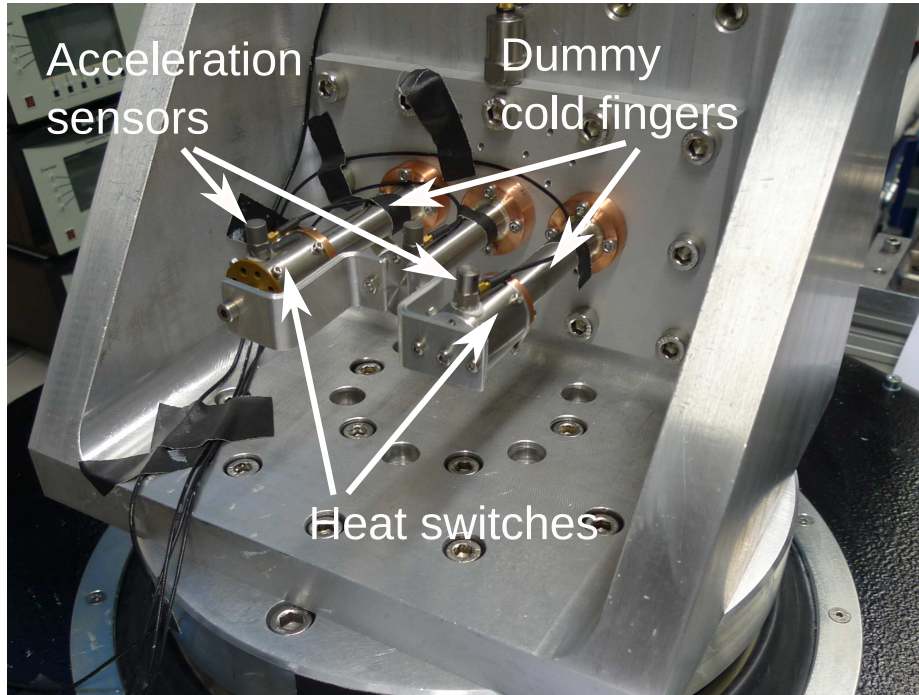


Figure 4: Test rig with two heat switches on the shaker (photo courtesy of AIM GmbH).

probably due to the contact area  $A$  that is smaller than assumed. That is, because of the structure of the switch, both switch halves may not press together everywhere with the same pressure, especially near the cold flange, where the jaws may not even touch the shaft. An increase in contact conductance is therefore anticipated when the contact between shaft and jaws is better aligned, e.g. by using a slightly conical shaft or flexibly attached jaws. As to be expected, the measured on-state conductance of 350 mW/K is lower than the 1000 mW/K reached in the previous project [4]. Besides the lower contact conductance  $h$ , the lower switch on-state conductance can also be attributed to the smaller switch dimensions and the use of aluminium instead of copper as the switch conduction material.

### 3. Stability

In order to verify the structural stability of the new switch design, it underwent a shaker test, which simulated the vibrations of a launch vehicle. For the test, two switches were mounted on a test rig simulating two cold fingers and a sensor carrier (see Fig. 4). The difference of the response curve at the beginning and at the end of the test showed almost no change, which proves that no structural damage occurred during this test. In addition, the switch thermal performance measured before and after the shaker test did not reveal any degradation.

The long-term stability was tested by measuring the temperature difference over the switch in closed state over a period of 6 months (see Fig. 5). For this test, the switch from the previous project [4] was used, which already underwent several dozens of cooling/warming cycles. Therefore, the switch can be regarded as “pre-aged”. In Fig. 5, the temperature difference  $\Delta T$  across the switch was monitored at a constant heat load of 1 W applied to the sensor side of the switch shaft. As seen from the Figure,  $\Delta T$  is stable or even

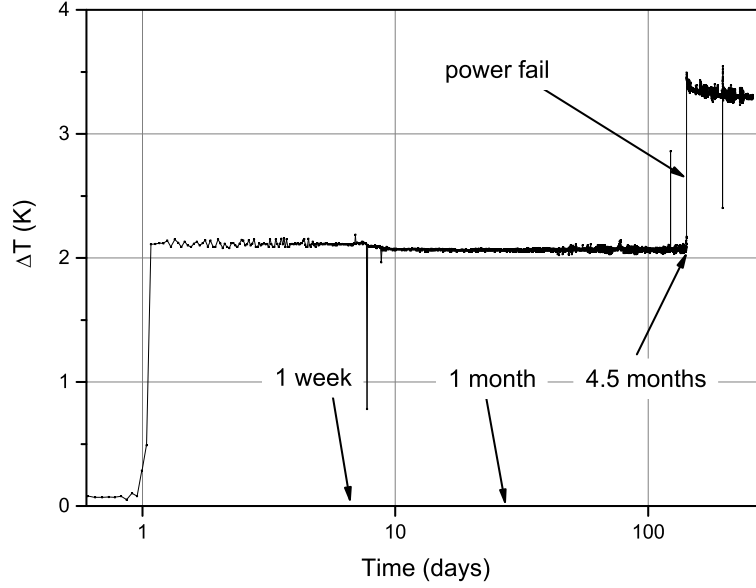


Figure 5: Long term measurement of the temperature difference across the switch of Ref. [4] at a heat load of 1 W. Cold flange temperature  $T_{CF} = 100$  K.

decreases a little bit for a period of more than 4 months. After 4.5 months, a power outage caused a vacuum pump failure and the switch warmed up at the same time. After power was restored, the switch was not able to return to its previous on-state performance. This behaviour may be caused by a contamination of the contact surface due to the vacuum leak. Besides this change in on-state performances, the switch showed no signs of degeneration over the initial 4 month of testing. A subsequent short term measurement over one month, which included a sudden heat-up to 200 K, showed no degeneration of the on-state conduction after the heat switch was cooled down to 100 K again. This means that pre-aging of the actuator material is an option to maintain stable long-term operation of this kind of thermal switch.

Another method to avoid creeping is to thermally anneal the thermoplastic material after machining has been finished. To evaluate this option, the UHMW-PE actuator of the newly designed switch was replaced by one, which was annealed at different temperatures. The switch was first cooled under its closing temperature and warmed up to room temperature again. This process was repeated several times and the closing/opening temperatures were monitored. When the actuator material was annealed using the UHMW-PE supplier's recommended thermal cycle between room temperature and 85°C, it showed severe degeneration in closing temperature as can be seen from Fig. 6a. The annealing temperature was then increased from 85°C to 105°C using a new actuator sample and this time the switch showed almost no change in opening/closing temperatures as shown in Fig. 6b. As expected, the on-state condition after the cyclic actuation stayed at its initial value of 250 mW/K at the beginning of the test cycle. Proper annealing is therefore an important process for gaining repeatable switch operation.

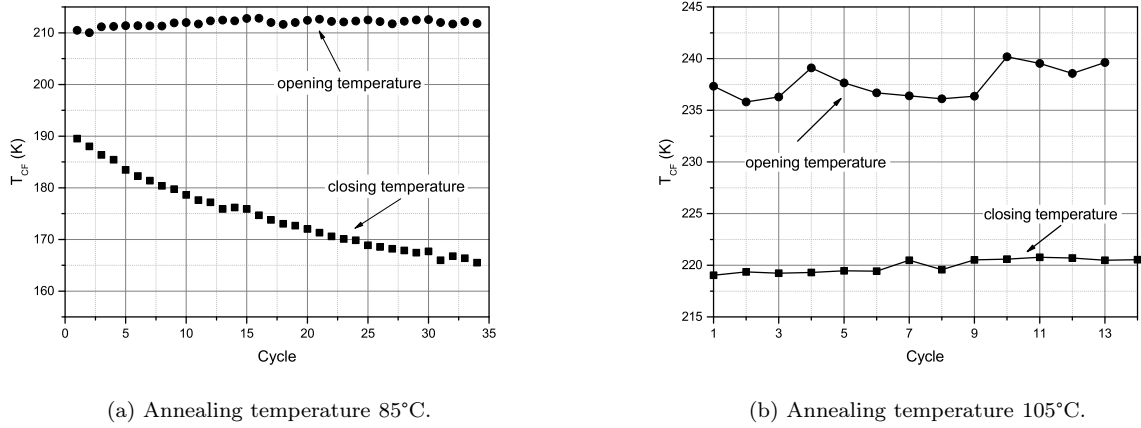


Figure 6: Open/Close-cycles of the new switch with different annealing temperatures of the UHMW-PE actuator.

#### 4. Conclusions

Using a combined thermo-mechanical model, the mass and the stability of a CTE-based heat switch was optimized. The mass of the new switch is only 25 g compared to 250 g of the previously realized switch [4]. The calculated thermal conductances are compared with experimental data. The predicted off-state conductance is higher than in the experiment due to additional contact resistances which are not included in the model. The predicted on-state conductance is lower than in the model, likely because of the imperfect contact area alignment. This gives rise for further improvement. The developed models enable the easy scaling of the switch dimensions to fulfil the requirements by a given application.

In contrast to the previous development, the mechanical and thermal stability of the heat switch is proven by shaker tests and long-term measurements. The next step will be the incorporation of the switch design in a practical space application.

#### Acknowledgements

This work was financially supported by the German Federal Ministry of Economics and Technology (BMWi Grant No. 50 EE 1322). The authors thank AIM Infrared Modules GmbH (Heilbronn) for performing the shaker tests. Useful discussions with Jan Grosser and Alexander Gerling (DLR Bonn) are gratefully acknowledged.

#### References

#### References

- [1] R. G. Ross, Cryocooler Reliability and Redundancy Considerations for Long-Life Space Missions, in: Cryocoolers 11, Springer Science + Business Media, 2001, pp. 637–648. doi:10.1007/0-306-47112-4\_79. URL [http://dx.doi.org/10.1007/0-306-47112-4\\_79](http://dx.doi.org/10.1007/0-306-47112-4_79)

- [2] R. G. Ross, Active Versus Standby Redundancy for Improved Cryocooler Reliability in Space, in: Cryocoolers 13, Springer Science + Business Media, 2005, pp. 609–618. doi:10.1007/0-387-27533-9\_76.  
URL [http://dx.doi.org/10.1007/0-387-27533-9\\_76](http://dx.doi.org/10.1007/0-387-27533-9_76)
- [3] K. Lankford, Spacecraft Thermal Control Handbook, Volume I: Fundamental Technologies, 2nd Edition, Vol. I, AIAA, 2002, Ch. 10, pp. 353–371.
- [4] M. Dietrich, A. Euler, G. Thummes, A compact thermal heat switch for cryogenic space applications operating near 100 K, Cryogenics 59 (2014) 70–75. doi:10.1016/j.cryogenics.2013.11.004.  
URL <http://dx.doi.org/10.1016/j.cryogenics.2013.11.004>
- [5] M. Bahrami, J. R. Culham, M. M. Yovanovich, Modeling Thermal Contact Resistance: A Scale Analysis Approach, J. Heat Transfer 126 (6) (2004) 896. doi:10.1115/1.1795238.  
URL <http://dx.doi.org/10.1115/1.1795238>
- [6] L. W. Yang, G. Thummes, Development of Stirling-Type Coaxial Pulse Tube Cryocoolers, in: Cryocoolers 13, Springer Science + Business Media, 2005, pp. 141–148. doi:10.1007/0-387-27533-9\_20.  
URL [http://dx.doi.org/10.1007/0-387-27533-9\\_20](http://dx.doi.org/10.1007/0-387-27533-9_20)
- [7] S. S. Kumar, K. Ramamurthi, Thermal contact conductance of pressed contacts at low temperatures, Cryogenics 44 (10) (2004) 727–734. doi:10.1016/j.cryogenics.2004.04.004.  
URL <http://dx.doi.org/10.1016/j.cryogenics.2004.04.004>